

Structural and Thermal Stability of B₄C/Ru Multilayers with Carbon Barrier Layers

A.V. Bugaev,^a S.S. Sakhonenkov,^a A.U. Gaisin,^a R.A. Shaposhnikov,^b V.N. Polkovnikov^b and E.O. Filatova^a

^a *Institute of Physics, St-Petersburg State University, Ulyanovskaya Str. 1, Peterhof, St. Petersburg 198504, Russia*

^b *Institute for Physics of Microstructure, Russian Academy of Sciences, Nizhny Novgorod 603087, Russia*

Abstract

The chemical interaction between Mo and Ru layers in multilayer structures depending on the thickness ratio (Γ) was carried out using X-ray photoelectron spectroscopy (XPS), X-ray diffraction (XRD) and X-ray reflectometry (XRR). The results showed significant interaction of materials inside multilayer structures with the formation of ruthenium borides, with an increase in the B₄C layer thickness (a decrease in the Γ parameter) leading to the formation of ruthenium borides of different stoichiometry. The introduction of a carbon barrier layer at the Ru-on-B₄C interface resulted in significant suppression of ruthenium boride formation. The thermal stability of the B₄C/Ru system was also studied upon annealing at 400 °C for 1 hour before and after the introduction of the carbon barrier layer. It was shown that the introduction of a carbon barrier layer at the Ru-on-B₄C interface increases the thermal stability of the system, which makes this system more suitable for use in optical systems exposed to long-term radiation. The obtained results are important for the development of highly efficient multilayer mirrors used in EUV lithography and X-ray optics.

Keywords: B₄C/Ru, multilayer structures, barrier layers, thermal stability, EUV lithography, X-ray optics.

Introduction

X-ray optics is one of the key technologies in various scientific, engineering and industrial applications such as lithography, high-resolution microscopy, X-ray fluorescence analysis, synchrotrons, free-electron lasers and space astronomy [1–3]. Among these, one of the most critical applications is next-generation lithography. In the microelectronics industry, there is an unceasing global trend of scaling down the manufacturing procedures to increase the operating frequency and decrease the power consumption, and of enhancing the computational capacity of microprocessors [4–6]. Thus, increasing the resolution of the lithography equipment employed in

the industry and the associated decrease in the working wavelength of the required light beam is the main technical route agreed upon by industry and science [7].

In fact, lithography at a wavelength of 6.6–6.7 nm (often referred to as Beyond Extreme Ultraviolet (BEUV) lithography) is a promising area of research that can stimulate further development of microchip technology, allowing the creation of more compact, more powerful and more efficient processors. Multilayer mirrors with high reflectivity play a crucial role in the technology of BEUV light management in lithography. This wavelengths range is attractive for the following reasons: firstly, the boron absorption K-edge lies just beyond this spectral range ($\lambda_k \sim 6.63$ nm). This makes it possible to use boron or its compounds as a weakly absorbing spacer in a multilayer mirror. Secondly, terbium and gadolinium-based light sources [8,9] can provide high system performance. Thirdly, in accordance with the Rayleigh criterion, the transition to this wavelength allows the resolution to be doubled compared to the actively developed lithography with an operating wavelength of 13.5 nm.

It should be noted that other important practical applications of multilayer X-ray mirrors optimized for a working wavelength of 6.7 nm include X-ray fluorescence analysis, which is a non-destructive method for studying various objects [10], such as ores, alloys, water-containing samples, bones and tissues [11,12]. In addition, multilayer X-ray mirrors are actively used as optical elements for synchrotron radiation sources, providing high-intensity monochromatization of the beam [13].

Multilayer structures considered for this wavelength range typically consist of lanthanum or molybdenum paired with B₄C [14–17]. However, theoretical analysis of the reflectance spectra in the wavelengths range from 6 to 9 nm of ideal multilayer X-ray mirrors composed of various materials, highlights the unique potential of multilayer structures based on carbon boride (B₄C) and ruthenium (Ru) [18–20]. These systems exhibit outstanding optical properties, making them highly attractive. Ru, as a material with a high atomic number (Z=44), has significant electron density, which is critical to achieving high reflectivity in the soft X-ray range. B₄C, in turn, is an ideal partner for Ru due to the optimal combination of low absorption and a suitable refractive index in the working spectral range.

The system's advantages include higher thermal stability and resistance to radiation exposure, which is especially important when working with powerful radiation sources. In [21–23] the effect of annealing on the reflectivity and internal stresses of multilayer Ru/B₄C structures were investigated. It was shown that the reflectivity remains almost unchanged during annealing up to 550 °C, while internal stresses were reduced during thermal annealing.

Despite the high theoretical values of the reflection coefficient, today there is a significant difference between the theoretically predicted and experimentally achieved values, which dictates the need for further thorough studies of the structure in order to identify the reasons for the discrepancy. According to theoretical calculations, the reflectivity of the B₄C/Ru multilayer structure in the wavelength range near to 6.7 nm reaches 70% [24], while the value of experimentally obtained reflectivity does not rise above 30% [25,26].

The main reason for the decrease in reflectivity is the formation of transition layers at the interfaces as a result of the interdiffusion of the main layers with the formation of new compounds [27]. These compounds significantly reduce the contrast of the interfaces and, as a consequence, the efficiency of interference reflection. Another important issue is the increase in interlayer roughness during the growth of the multilayer structure [28]. The accumulation of roughness from layer-to-layer leads to an increase in radiation scattering and a decrease in reflection coherence. Also, the internal stresses found in the B₄C/Ru system, reaching a value of -950 MPa [18], also negatively affect the state of the interfaces between the main layers, as a result, reducing the optical characteristics of these multilayer mirrors.

To overcome the problem of interaction of the layers in multilayer structures, the method of introducing barrier layers at the interfaces is actively used [29,30]. The concept of a barrier layer involves the deposition of an ultra-thin layer (of the order of several angstroms) of material that inhibits interdiffusion between the base layers. In addition, barrier layers can neutralize internal stresses arising in a multilayer structure, which also has a positive effect on the state of the interfaces [18]. With the correct choice of barrier layer material and the interface at which it is introduced, the approach allows maintaining the sharpness of the interfaces, reducing the formation of transition layers and increasing the reflectivity of the structure.

The aim of this work is to study multilayer B₄C/Ru structures obtained by magnetron sputtering. The main attention is paid to the analysis of the formation of interfaces in the system and the influence of the parameter Γ (the ratio of the thickness Ru to the period of the structure) on the composition of the transition layer. The prospects for practical application of B₄C/Ru systems are largely related to solving the problem of their long-term stability under operating conditions. Therefore, the thermal stability of the multilayer structure during high-temperature annealing is also studied. The effect of introducing an ultrathin (0.3 nm) C barrier layer at the Ru–B₄C interface is also studied. The results obtained in this work are important for optimizing B₄C/Ru mirrors in EUV lithography and X-ray optics.

2. Experimental

All samples were synthesized by direct current magnetron sputtering using the laboratory setup described in the work [31]. Deposition was performed on high-purity super polished Si(100) substrates with an RMS roughness of 0.2 nm in the spatial frequency range of 0.025 – 64 μm^{-1} . Before deposition, the pressure of the residual gases in the chamber did not exceed $5 \cdot 10^{-7}$ Torr. During the sputtering process, argon with a purity of 99.998% was used at a working pressure of $2.48 \cdot 10^{-3}$ Torr. Discharge parameters during deposition and the rate of layer growth for the studied multilayer structures are shown in Table 1. The thickness of the layers was controlled by adjusting the speed of the substrate passing over a stationary target.

Multilayer structures are denoted by the formula $[X/Y/Z]_n$, where X, Y, Z are materials of the layers, and n is the number of periods of the structure. The period denotes the total thickness of a group (in base case a pair) of alternating layers. In this notation, the leftmost element (X) corresponds to the layer located closer to the substrate, and the rightmost element (Z) corresponds to the layer located closer to the surface.

Table 1. Discharge parameters during deposition and the rate of layer growth.

Structure of sample	Material	Voltage, V	Current, mA	Growth rate, nm/s
$[\text{B}_4\text{C}(2.61)/\text{Ru}(0.78)]_{50}$	Ru	248	300	0.03
	B_4C	260	1200	0.02
$[\text{B}_4\text{C}(1.75)/\text{Ru}(1.44)]_{50}$	Ru	238	300	0.035
	B_4C	268	800	0.015
$[\text{B}_4\text{C}(1.86)/\text{C}(0.3)/\text{Ru}(1.29)]_{50}$	Ru	305	300	0.1
	B_4C	299	800	0.02
	C	312	500	0.13

The chemical composition of the multilayer structures was studied by X-ray photoelectron spectroscopy (XPS) at the ESCA laboratory module located at the NANOPES station of the Kurchatov Center for Synchrotron Radiation and Nanotechnology. X-ray photoelectron spectroscopy is a non-destructive method for analysis of the elemental composition, as well as the electronic and chemical state of atoms located in the near-surface region of the material under investigation [32,33]. The spectrometer is equipped with hemispherical energy analyzer PHOIBOS HSA 3500 with a diameter of 150 mm, mounted at an angle of 45° to the direction of the X-ray beam. Monochromatized X-ray radiation from an X-ray tube with an aluminum anode ($\text{Al } K\alpha$, $h\nu = 1486.6$ eV) with an energy resolution better than 0.4 eV is used as the radiation source. The energy calibration of the spectra was performed using the Fermi level, bringing the

inflection point to zero. In addition, the spectrometer is equipped with an Ar^+ ion gun, which enables to clean sample surface from carbon and oxygen contaminations. When processing the data, the contribution of the inelastic scattering background was taken into account using the universal Tougaard function [34,35]. For a better interpretation, some of the photoelectron spectra were decomposed into components using the Casa XPS software [36].

Data on the crystal structure, layer thickness, and characteristics of the interfaces were obtained by analyzing the results of X-ray diffraction (XRD) and X-ray reflectometry (XRR). The measurements were carried out at a Bruker D8 Discover laboratory diffractometer of the “Research Centre for X-ray Diffraction Studies” of Saint Petersburg State University. The experimental setup includes an X-ray tube with a copper anode and a high-precision horizontal goniometer, which provides scanning in $\theta - 2\theta$ geometry with a sample positioning accuracy of 50 μm and an angular resolution of 0.001°. Theoretical calculations and fitting of experimental reflection curves were performed using the IMD [37] and Multifitting software [38].

3. Results and discussion

3.1 Reference structures

As a result of chemical interactions between the main layers in the multilayer $\text{B}_4\text{C}/\text{Ru}$ structures, the formation of ruthenium (carbo-)borides can be expected. To date, no reports have been found in the literature describing the formation of ruthenium carbo-borides RuB_xC_y in $\text{B}_4\text{C}/\text{Ru}$ systems, while the formation of ruthenium borides has been observed in previous studies [27,28]. Table 2 summarizes the formation energies of several known ruthenium borides and carbides, as well as B_4C obtained from the Materials Project database [39] and from the literature [40]. The data clearly show that Ru-C compounds are thermodynamically unstable under ambient conditions. Among the borides, RuB_2 and Ru_2B_3 have the most negative formation energies indicating a higher driving force for their formation.

To further assess the likelihood of interfacial product formation, we employed an interface reaction analysis approach similar to that described in [41] and [42], where the thermodynamic driving force for reaction between two solids is evaluated from bulk phase data using convex-hull phase diagrams. In this formalism, all possible reactions between B_4C and Ru were enumerated within the compositional space $\{\text{B}, \text{C}, \text{Ru}\}$, and the most exergonic product set was identified. Despite the high intrinsic stability of B_4C , the calculations indicate a strong thermodynamic tendency for it to react with Ru to form Ru_2B_3 and elemental carbon. The reaction energy is negative (-0.352 eV/atom) relative to the stable phases of Ru and B_4C , which implies that the

formation of Ru_2B_3 at the interface is energetically favorable. Therefore, in the studied systems it is reasonable to expect the occurrence of ruthenium boride phases at the $\text{B}_4\text{C}/\text{Ru}$ interfaces.

Table 2. Formation energies for ruthenium borides.

Borides	RuB	RuB_2	Ru_2B_3	Ru_7B_3	RuC	Ru_2C	B_4C
Formation energy (eV/atom)	0.801	-0.308	-0.352	-0.142	0.649	0.950	-0.647

To study the processes occurring in multilayer $\text{B}_4\text{C}/\text{Ru}$ structures, it is necessary to consider the XPS spectra of reference structures. Ru and B_4C films were used for this purpose.

Figure 1a shows the decomposition of Ru $3\text{d}_{5/2}$ photoelectron spectrum obtained from the reference 10 nm pure Ru film after surface cleaning with Ar^+ ions. Here and below, when the spectra are decomposed into components, the measured spectrum is shown by black dots, and the red line shows the curve representing the sum of the components of the decomposition. Since the Ru $3\text{d}_{3/2}$ peak strongly overlaps with the C 1s peak of an adventitious carbon and is considerably separated from the Ru $3\text{d}_{5/2}$ peak by about 4.2 eV, only the Ru $3\text{d}_{5/2}$ line will be analyzed here and below. The Ru $3\text{d}_{5/2}$ photoelectron peak measured for the reference Ru has energy position 279.9 eV and the full width at half maximum (FWHM) 0.4 eV, which correlates well with the literature data [43,44].

Figure 1b shows the B 1s photoelectron spectrum measured for the reference B_4C film. Boron carbide has a complex structure made up of C-B-C chains and B_{12} or B_{11}C icosahedra [45,46]. As a result, the spectrum includes both B-B and B-C bonds. The spectrum decomposition shows that the main peak is a combination of two components: one at 188.4 eV (FWHM = 1.8 eV) corresponding to B-B bonds, and another at 189.7 eV (FWHM = 1.9 eV) corresponding to B-C bonds [47,48]. A small peak from boron oxide is also visible at 191.2 eV.

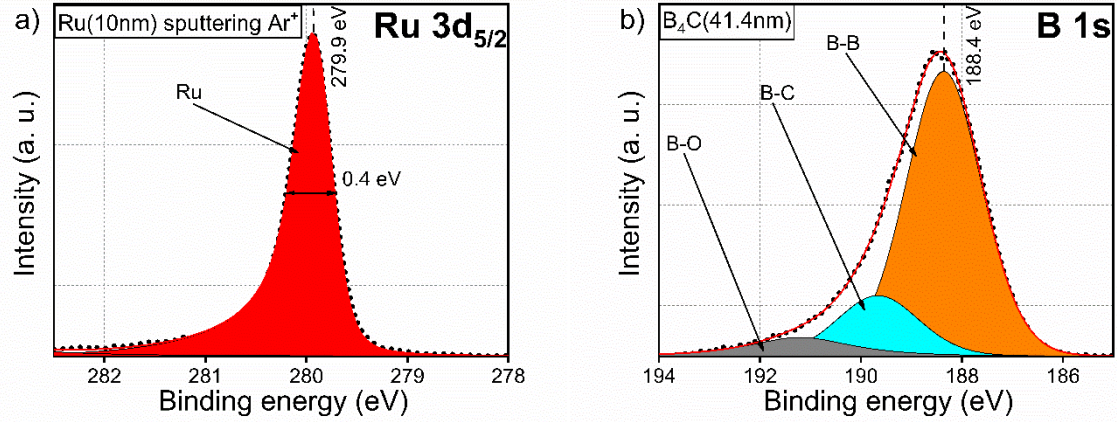


Figure 1. Decomposed Ru 3d_{5/2} and B 1s photoelectron spectra obtained from reference Ru(10nm) (a) and B₄C(41.4 nm) (b) films.

3.2 B₄C/Ru multilayer structures with different Γ

Particular attention should be paid to the parameter Γ , which determines the ratio of the thickness of the strongly absorbing material (ruthenium) to the thickness of the structure period d. By decreasing the thickness of the absorbing layer and increasing the thickness of the less absorbing one within a fixed value of the parameter, it is possible to reduce the overall absorption losses while maintaining high reflectivity of the system. However, it should not be forgotten that too large decrease in the thickness of the absorbing layer will lead to deterioration of the interference. The balance is achieved at some intermediate values of Γ [49,50]. It is also worth remembering that the mutual diffusion between the layers can also be different at different ratios of the layer thicknesses in systems with the same period value. Changing the parameter Γ can also affect the transverse and columnar roughness in a multilayer system [49,51]. Thus, studying structures with different Γ parameters is important to determine the optimal Γ value that minimizes interface imperfections and also reduces absorption. In this regard, two multilayer systems consisting of 50 periods with a nominal period thickness of about 3.3 nm and Γ parameters equal to 0.23 and 0.45, respectively, were analyzed.

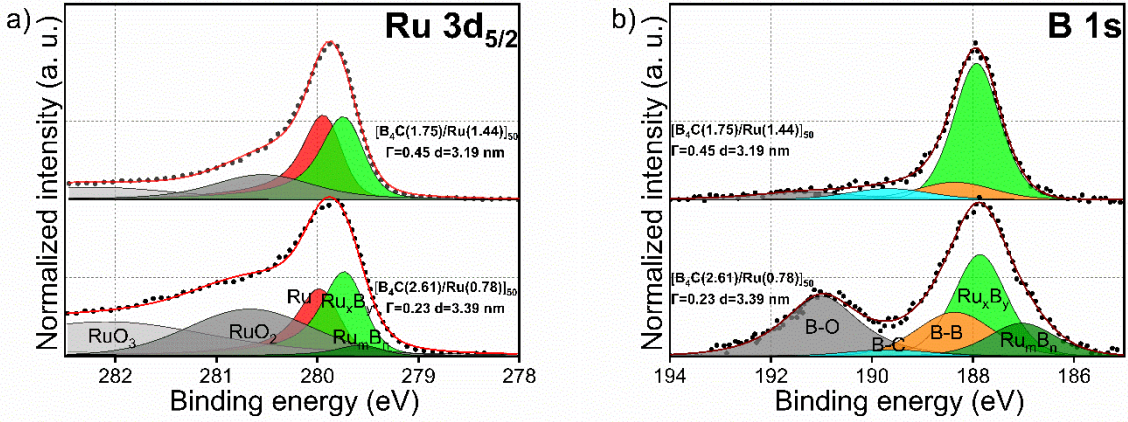


Figure 2. Decomposed Ru 3d_{5/2} (a) and B 1s (b) photoelectron spectra obtained from [B₄C/Ru]₅₀ multilayer systems with $\Gamma = 0.23, 0.45$.

The decomposition of the Ru 3d_{5/2} and B 1s photoelectron spectra obtained for the multilayer structures [B₄C/Ru] with $\Gamma = 0.23, 0.45$ is presented in Figure 2. The line shape, energy position and FWHM of the peaks obtained for the reference Ru and B₄C were rigidly fixed and used in the decomposition of the spectra of the multilayer structures. Here and below, all photoelectron spectra were normalized to peak intensity for the comparison convenience.

Since XPS is a surface sensitive technique, it is important to estimate the photoelectron escape depth in the systems under consideration. In accordance with the methodology described in the article [52], the depth at which 95% of the useful signal is formed (information depth) in the [B₄C(1.75 nm)/Ru(1.44 nm)]₅₀ system with $\Gamma = 0.45$ is estimated to be approximately 7.7 nm for the B 1s line and 7.4 nm for the Ru 3d line. Since the period of the system is 3.19 nm, it can be assumed that the measured photoelectron spectra carry information from more than two periods. Crucially, spectra contain contributions from both interfaces: Ru-on-B₄C and B₄C-on-Ru.

Analysis of the decomposed Ru 3d_{5/2} photoelectron spectrum of the multilayer structure [B₄C(1.75 nm)/Ru(1.44 nm)]₅₀ indicates the appearance of an additional component from the side of lower binding energies relative to pure ruthenium ($E = 279.7$ eV), which indicates the formation of an additional compound Ru_xBy as a result of the interaction of the Ru and B₄C layers. The presence of a shoulder on the side of high binding energies indicates contributions to the spectrum from oxide components. It should be emphasized that due to the small thickness of the main layers, the multilayer structures were not exposed to Ar⁺ ion sputtering. It is known [53–55] that cleaning with an ion beam can potentially lead to preferential sputtering with significant redistribution of number of atoms within the sample and additional mixing of the layers. Therefore, keeping surface intact in this system is reasonable. The spectrum decomposition indicates the presence of two additional components. The first component is located at a binding energy of 280.5 eV and can be

referred to RuO_2 [43,56–59] and the second one is centered at the 282.3 eV and can be assigned to RuO_3 [43,59–61].

Analysis of the B 1s spectrum of the multilayer $[\text{B}_4\text{C}(1.75 \text{ nm})/\text{Ru}(1.44 \text{ nm})]_{50}$ structure (Fig. 2b) indicates a significant decrease in the intensities of the lines associated with the B-B and B-C bonds and the appearance of a fairly narrow, high-intensity line on the side of lower binding energies in relation to the B-B component, at a binding energy of 187.6 eV. Since in the literature [47,62,63] the peaks of metal borides in B 1s spectra are mostly located at lower binding energies relative to the peak corresponding to the B-B bond, it is reasonable to assume that in the spectrum under consideration the high-intensity peak also reflects the formation of the Ru_xB_y compound. The appearance of a peak associated with formation of the borides on the side of lower energies in both the Ru 3d_{5/2} and B 1s spectra is noteworthy. The analysis of the energy position of the peak makes it possible to draw conclusions about the chemical state of the atom in a compound, since the peak position changes depending on the type of surrounding atoms and the nature of chemical bonding. Chemical shifts are primarily caused by the redistribution of the valence electron density when an atom participates in chemical bonding, which directly affects the binding energy of core levels. Different binding energies of electronic levels reflect their charge state in the compound, and significant differences in these values characterize the direction of electron transfer from a less electronegative atom to a more electronegative one. [62,64], in which the shift in binding energy observed in the spectrum is mainly due to a relaxation shift, while the charge transfer in this case is negligible. The relaxation shift can significantly prevail over the chemical shift, resulting in the binding energy shift in the spectrum being mainly determined by the relaxation shift. This preserves the direction of the peak shift in the spectrum, i.e., the peaks reflecting the formation of a compound in the spectra of different components shift in the same direction. It can be assumed that the shift in the binding energy in the Ru 3d_{5/2} spectrum is mainly due to the relaxation shift, and that the charge transfer in this case is insignificant.

Also, the $[\text{B}_4\text{C}(2.61 \text{ nm})/\text{Ru}(0.78 \text{ nm})]$ multilayer structure with $\Gamma = 0.23$ was studied. The calculation of the information depth for this system showed a value of 9.3 nm for the B 1s line and 8.9 nm for the Ru 3d line with a period value of 3.39 nm. Thus, it can be stated that the spectra obtained from this sample also contain contributions from both the Ru-on-B₄C interface and the opposite B₄C-on-Ru interface. The joint analysis of the Ru 3d_{5/2} and B 1s spectra (Fig. 2) of this system indicates the appearance of an additional low-intensity component in both spectra, which can be attributed to the formation of ruthenium boride as well, but with a different stoichiometry Ru_mB_n . The additional ruthenium boride Ru_mB_n is located at an even lower binding energy than Ru_xB_y . A stronger shift of the corresponding component towards lower binding energies means a

higher electron density on boron, i.e. boron becomes more strongly hybridized with ruthenium. This condition manifests itself in a large number of boron-containing compounds that form complex polyhedral clusters around the metal [65,66].

The significant increase in boron oxide compared to the multilayer structure with the parameter $\Gamma = 0.45$ is noteworthy. It can be assumed that the ruthenium layer of thickness 0.78 nm does not protect the system from oxygen penetration into the structure.

A joint analysis of the spectra obtained from multilayer $\text{B}_4\text{C}/\text{Ru}$ structures with different Γ shows that the sample with a thinner Ru layer thickness (smaller Γ) is prone to the formation of ruthenium borides of different stoichiometry at the interface.

3.3 System with barrier layer

One of the perspective ways to limit the formation of transition layers is to apply a thin barrier layer at the interface between the main layers. The use of barrier layers not only reduces the mutual diffusion of the main layers, but also increases the reflectivity by reducing the roughness of the interfaces, as well as improving thermal and radiation stability [26,67]. The material used as a barrier layer must itself have good thermal stability, adhesion, and optical constant values in the operating energy range for a given multilayer mirror.

Carbon was used as the barrier layer material in this work. The use of carbon barrier layers in multilayer X-ray mirrors is a widely adopted practice. It has previously been shown that carbon promotes the smoothing of interfacial boundaries and reduces interdiffusion of the components [68–71]. In this study, the carbon interlayer is applied only at one of the interfaces. In the spectral region near the absorption edge, the empirical Larruquet rule [72,73] is fulfilled, according to which the maximum reflectance of a multilayer structure is achieved for a specific sequence of materials.

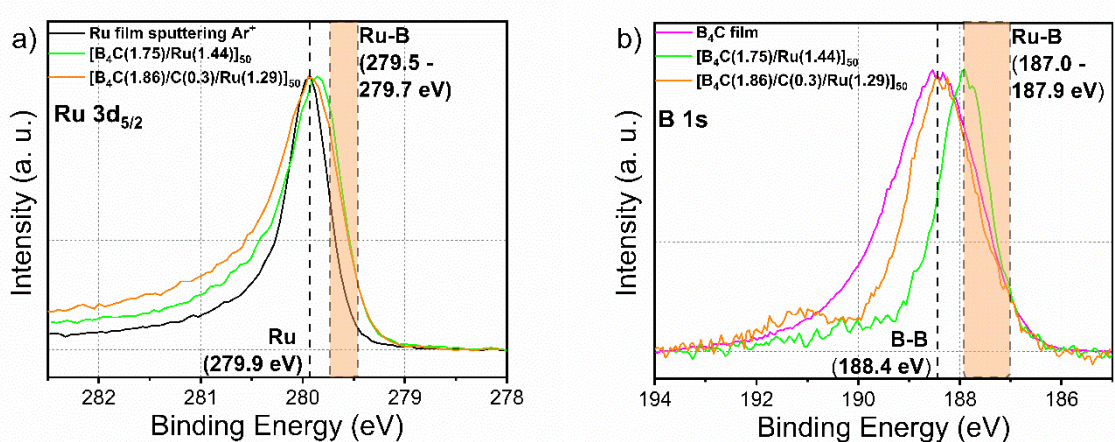


Figure 3. Ru 3d_{5/2} (a) and B 1s (b) photoelectron spectra collected from the [B₄C(1.75 nm)/Ru(1.44 nm)]₅₀, [B₄C(1.86 nm)/C(0.3 nm)/Ru(1.29 nm)]₅₀ multilayer systems and Ru, B₄C reference films.

Figure 3 show the photoelectron spectra of Ru 3d_{5/2} and B 1s, respectively, obtained from the [B₄C(1.86 nm)/C(0.3 nm)/Ru(1.29 nm)]₅₀ and [B₄C(1.75 nm)/Ru(1.44 nm)]₅₀ multilayer structures and Ru, B₄C reference films. The joint analysis of the Ru3d_{5/2} spectra indicates a broadening of the main peak toward higher binding energies in the spectra of the system with the barrier layers compared to the spectrum of the system without barrier layers. In the B 1s spectrum of the system with the barrier layer, the main line exhibits not only broadening but also a noticeable shift. The broadening of the Ru 3d_{5/2} peak and the shift accompanied by broadening of the B 1s peak in the system with the barrier layer can be attributed to an increased contribution from pure Ru and B₄C, as indicated by the positions of the corresponding reference peaks. One can conclude that the introduction of the C barrier layer into B₄C/Ru multilayer structure quite effectively prevents mixing of the main layers and, therefore, significantly reduces the formation of the ruthenium boride compound.

3.4 Effect of high-temperature annealing

As noted in the introduction, the main application field of B₄C/Ru multilayer mirrors is optical systems for EUV lithographers. Since some mirrors in the optical systems are exposed to X-ray and extreme ultraviolet radiation of high intensity (up to 250 W [6]) for a long time, they can be subjected to severe thermal load. Heating of optical elements can lead to undesirable disruption of periodicity of multilayer structures due to mixing of layers, crystallization, etc. and, as a consequence, reduce their reflectivity. Therefore, mirrors in EUV lithographs must be heat resistant, i.e., withstand long-term exposure to high temperatures without substantial changing their original characteristics. Additionally, annealing the multilayer structure at high temperatures enhances the intermixing of the main layers, which allows one to study the diffusion properties of atoms in a multilayer coating.

Despite the fact that some studies [22,23] report minimal changes in the reflectivity of multilayer B₄C/Ru mirrors during annealing up to 550 °C, other authors [74] report that already at a temperature of 490 °C, a sharp degradation of the multilayer structure occurs, which is accompanied by a strong decrease in reflectivity. Thus, the question of the thermal stability of the B₄C/Ru structure remains open. The authors of the work [74] claim that at a temperature of 400 °C, the thickness of the transition junctions at the interfaces begins to grow. However, a catastrophic loss of reflective properties has not yet occurred. Thus, 400 °C is the "threshold"

temperature for studying the initial stages of degradation of the B₄C/Ru structure. Based on these data, the [B₄C(1.75)/Ru(1.44)]₅₀ system with $\Gamma = 0.45$ and $d = 3.19$ nm was annealed at 400 °C for 1 hour to study thermal stability at this temperature.

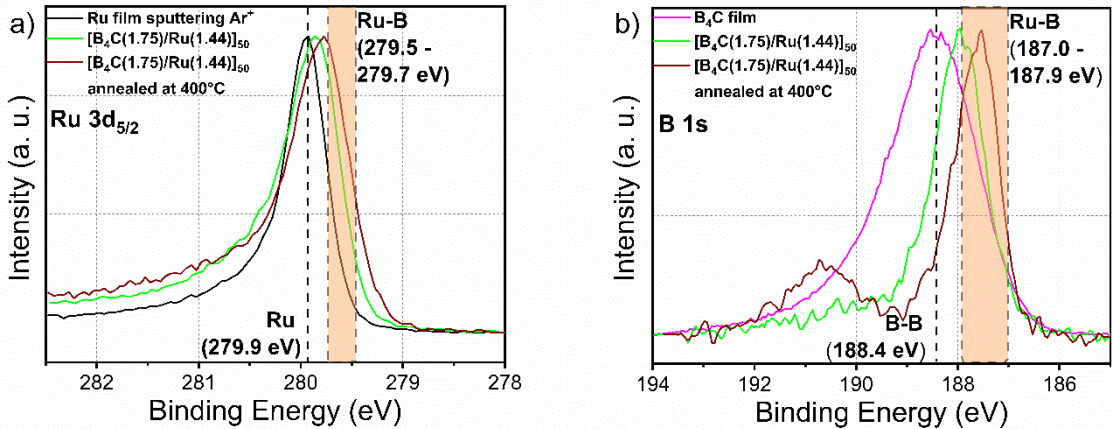


Figure 4. Ru 3d_{5/2} (a) and B 1s (b) photoelectron spectra collected from the Ru and B₄C reference films and [B₄C(1.75 nm)/Ru(1.44 nm)]₅₀ multilayer system before and after annealing at 400 °C.

Figure 4a shows the Ru 3d_{5/2} photoelectron spectra measured from [B₄C(1.75 nm)/Ru(1.44 nm)]₅₀ multilayer system before and after annealing, as well as the spectrum of the reference Ru film. It can be seen that annealing at 400 °C affects the shape and position of the main peak. In particular, there is a noticeable shift and broadening of the main peak towards lower binding energies. This fact indicates active mixing of the main layers during thermal annealing and, as a result, more active formation of Ru-B bond. Similar trend (without broadening) is observed in the B 1s spectra presented in Figure 4b, also indicating increased intermixing of the main layers in the annealed multilayer structure. A strong shift of the B 1s peak towards lower binding energies by 0.4 eV is traced in the B 1s spectrum of the annealed multilayer structure confirming the formation of great amount of the ruthenium boride. Also, a noticeable growth of the boron oxide peak is observed in the B 1s spectrum, which indicates active oxygen movement deep into the structure under the Ru surface layer.

It can be concluded that annealing at 400 °C for an hour enhances the mixing of layers, increasing the content of the formed ruthenium boride. The multilayer structure Mo/B₄C, which is also often considered as a system for use in lithography, has a significantly higher thermal stability [75,76].

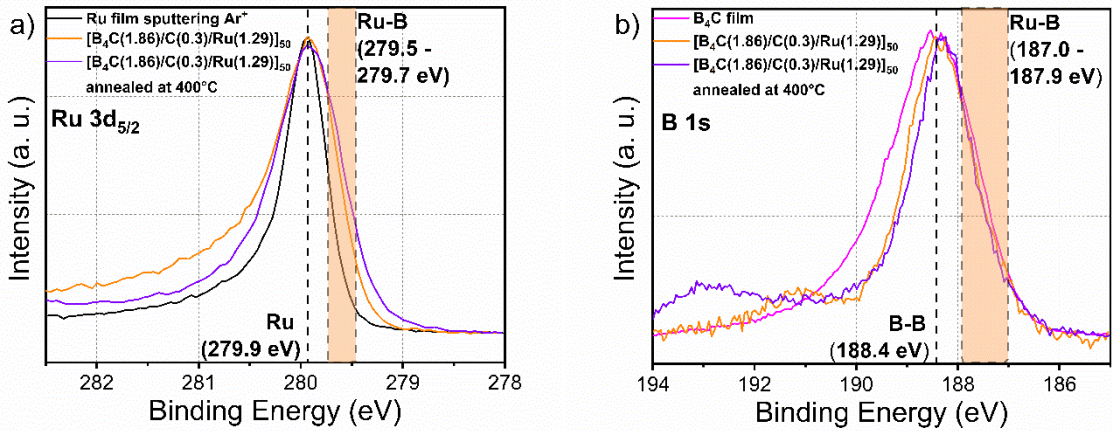


Figure 5. Ru 3d_{5/2} (a) and B 1s (b) photoelectron spectra collected from Ru and B₄C reference films and [B₄C(1.86 nm)/C(0.3 nm)/Ru(1.29 nm)]₅₀ multilayer system before and after annealing at 400 °C.

The introduction of a thin C barrier layer 0.3 nm thick on the Ru-on-B₄C interface completely changes the situation. The [B₄C(1.86 nm)/C(0.3 nm)/Ru(1.29 nm)]₅₀ sample with was also annealed at a temperature of 400 °C for 1 hour. Figure 5a shows Ru 3d_{5/2} photoelectron spectra obtained from pure reference Ru, as well as the [B₄C(1.86 nm)/C(0.3 nm)/Ru(1.29 nm)]₅₀ system before and after annealing. Despite the formation of a slightly higher intensity shoulder at the main peak from the lower binding energies after annealing, there is no noticeable shift of the peak towards lower binding energies. Thus, it can be seen that in the B₄C/Ru system with the C barrier layer, in contrast to the system without a barrier layer, annealing at a temperature of 400 °C does not lead to the increased formation of ruthenium boride. The analysis of B 1s photoelectron spectra (Figure 5b) confirms the conclusions reached. Unlike a sample without a barrier layer, in which, after annealing, there was a strong shift of the main peak towards lower binding energies, there is no noticeable shift of the main peak in the system with the barrier layer.

It is worth noting the behavior of ruthenium and boron oxides components in the spectrum of this system. During annealing, the intensity of the shoulder of the main Ru 3d_{5/2} peak from high binding energies, which indicates the presence of RuO₂ and RuO₃ oxides, decreases. At the same time, a 1.5 eV shift of the oxide peak towards higher binding energies is observed in the B 1s spectrum. This effect can be explained by the fact that during annealing, oxygen previously bound to ruthenium migrates to more underlying layers and binds to boron. Thus, a boron oxide with higher oxygen content is formed in the structure after annealing, which is manifested in a higher binding energy of this peak.

Thus, it can be concluded that the system with the barrier layer is more thermally stable than a multilayer structure without the barrier layer. If annealing at 400 °C in the system without

the barrier layer leads to its noticeable degradation, then in the system with a barrier layer, similar annealing practically does not affect the state of the interfaces.

3.5 XRD and XRR results

Diffraction patterns were obtained for all the structures studied to determine the presence/absence of crystallization in the samples (Figure 6). For clarity, the diffraction curves have been shifted vertically. Crystallization can negatively affect the reflectivity of multilayer mirrors. Crystalline materials, as a rule, exhibit anisotropy of growth, which leads to heterogeneity of the layers. On the other hand, amorphous structures tend to have smoother and sharper layer boundaries. Thus, it is important to preserve amorphous structures. All the peaks observed in Figure 6 relate exclusively to the silicon substrate. Thus, it can be concluded that all structures retain an X-ray amorphous state.

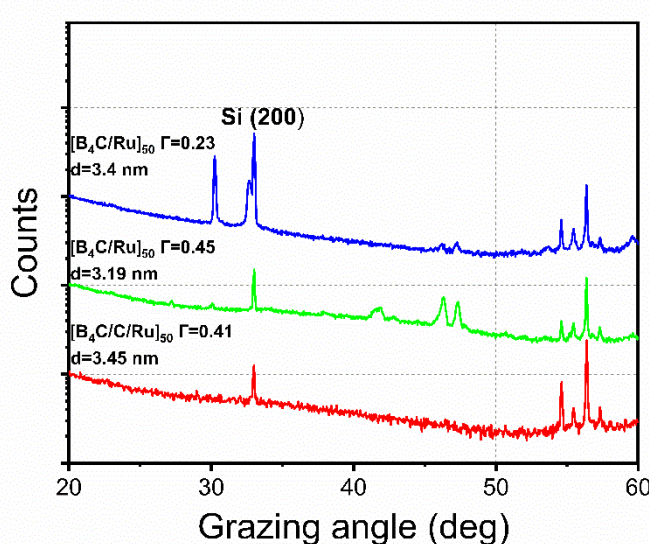


Figure 6. Diffraction patterns measured for the studied $\text{B}_4\text{C}/\text{Ru}$ (without and with C barrier layer) multilayer structures.

To determine the thickness of the main and transition layers, in all studied multilayer structures the measurements using X-ray reflectometry (XRR) were performed. Figure 6 shows the experimental (black dots) and fitted (red lines) reflection curves. For better visual perception, the reflection curves were shifted vertically. The captions of curves in the figure indicate the nominal values of the periods (d) and parameters of Γ .

A theoretical model was constructed based on the X-ray photoelectron spectroscopy data discussed above to fit the experimental curves. The models took into account surface layers containing oxygen (in the form of Ru and B oxides) and carbon contaminants, which required the subsurface region to be considered separately from the underlying layers, represented as a periodic

structure. In the multilayer system, the variation in layer thickness (Δz) with increasing period number, caused by the heterogeneity of deposition during growth, was taken into account. To describe the interlayer transition regions, a parameter s was introduced, combining the contributions of geometric roughness (including growth roughness) and mixing zones with the formation of the ruthenium boride. Various physical processes in the mixed regions were modelled by different functional dependencies: interdiffusion between the main layers was approximated by an error function, while mixing caused by energetic particle bombardment during sputtering was described by a linear dependence. Geometric roughness was described by an exponential function [77]. During the optimisation of the model parameters, the densities of the materials were fixed in accordance with the reference values from the Springer Materials database and were not varied [78]. Figure 7 shows the results of adjustments of the theoretical curves to the experimentally obtained results for $\text{B}_4\text{C}/\text{Ru}$ samples with different parameter Γ , as well as with the introduced barrier layer C. Table 4 shows the approximation parameters obtained for the samples presented.

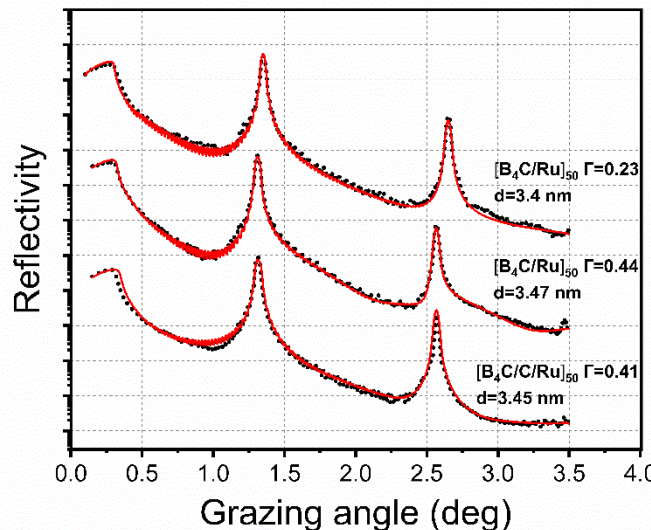


Figure 7. Experimental reflectance curves (black dots) and corresponding approximations (red lines) for the multilayer structures $[\text{B}_4\text{C}/\text{Ru}]$.

Table 4. Fitting parameters for the models of the multilayer samples (ρ – density, z - layer thickness, Δz – thickness drift, d – period thickness, Γ - ratio of z_{Ru} to d , s – transition region thickness (includes roughness and diffuseness)).

Layer	N	ρ , g/sm ³	z, nm	Δz , %	s, nm
$[\text{B}_4\text{C}/\text{Ru}]_{50}$ $d = 3.4$ nm, $\Gamma = 0.23$					
RuO_2	1	6.97	0.3		0.06
Ru	1	12.3	0.48		0.05

B ₂ O ₃	1	1.85	0.6		0.6
B ₄ C	1	2.51	2.01		1.2
Ru	49	12.3	0.92	0.53	0.4
B ₄ C		2.51	2.43	-0.22	0.5
[B ₄ C/Ru] ₅₀ d = 3.47 nm, Γ = 0.44					
RuO ₂	1	6.97	0.83		0.7
Ru	1	12.3	0.69		0.53
B ₂ O ₃	1	1.85	1.5		0.12
B ₄ C	1	2.51	0.44		0.39
Ru	49	12.3	1.37	0.98	0.36
B ₄ C		2.51	2.1	-0.65	0.47
[B ₄ C/C/Ru] ₅₀ d = 3.45 nm, Γ = 0.41					
RuO ₂	1	6.97	0.1		0.1
Ru	1	12.3	1.31		0.38
C	1	1.7	0.31		0.05
B ₂ O ₃	1	1.85	0.3		0.05
B ₄ C	1	2.51	1.44		1.2
Ru	49	12.3	1.53	0.29	0.12
C		1.7	0.3	0.01	0.25
B ₄ C		2.51	1.64	-0.27	0.25

As can be seen from Table 4, the values of parameter s for the B₄C and Ru layers show a significant difference in the transition layer thicknesses between the near-surface period and the main multilayer structure in all samples studied. This discrepancy may be due to the ambiguity of the solutions to the inverse reflectometry problem, which means that the fitting parameters must be interpreted with caution. Nevertheless, a clear systematic dependence is observed: for two samples with different values of Γ , the parameter s in the multilayer part of structures remains practically constant, amounting to $\sim 0.47 - 0.5$ nm for B₄C and $\sim 0.36 - 0.4$ nm for Ru. This suggests that the variation in the Γ parameter does not have a significant effect on the thickness of the mixed layer and roughness in the B₄C/Ru system. A comparison of the sample with $\Gamma = 0.44$ and the sample with a carbon barrier layer ($\Gamma = 0.41$) revealed a decrease in the s parameter by $0.22 - 0.24$ nm for both materials after the introduction of the barrier layer. The results obtained indicate a positive effect of the carbon barrier layer, leading to a decrease in both the thickness of the interface regions and the roughness value.

4. Conclusion

A comprehensive study of multilayer B₄C/Ru structures with different parameters Γ have been carried out using X-ray photoelectron spectroscopy (XPS), X-ray diffraction (XRD) and X-ray reflectometry (XRR).

Active interaction of the main layers in the system with the formation of ruthenium borides has been established, and an increase in the thickness of the B₄C layer (a decrease in the Γ parameter) leads to the formation of ruthenium borides of different stoichiometry. A ruthenium layer of thickness 0.78 nm does not protect the B₄C layer from oxidation.

The introduction of an ultrathin (0.3 nm) carbon barrier layer at the Ru-on-B₄C interface leads to a significant redistribution of the peak intensities of the components responsible for metallic Ru (in the Ru 3d_{5/2} spectrum) and B-B and B-C bonds (in the B 1s spectrum), which indicates an inhibition of the formation of ruthenium boride.

The thermal stability of the B₄C/Ru system was studied during annealing at 400 °C for 1 hour before and after the introduction of the C barrier layer. The results of the XPS studies of the multilayer structure without a barrier layer showed a significant increase in the mutual diffusion of the layers, accompanied by an increase in the thickness of the mixing regions and oxidation of the surface layers. This indicates a limited thermal stability of the B₄C/Ru structure. The introduction of a C barrier layer on the Ru-on-B₄C interface increases the thermal stability of the system. Annealing at 400 °C leads only to a redistribution of oxygen in the system. Thus, the use of multilayer B₄C/Ru systems with a barrier layer is preferable in optical systems exposed to prolonged radiation exposure.

The analysis of the XRD curves shows the X-ray amorphousness of all the studied samples. The analysis of reflection curves by the XRR method reveal a decrease in the parameter s (thickness of the transition region) by 0.22–0.24 nm in the system with barrier layer.

The results obtained are important for the development of highly efficient multilayer mirrors used in EUV lithography and X-ray optics. This work demonstrates the prospects of using B₄C/Ru systems with a carbon barrier layer to minimize the effects of the interaction of the main layers and the formation of sharp interfaces in these structures to create high-quality optical elements.

Funding sources

Russian Science Foundation Grant No. 19-72-20125-II.

Acknowledgements

This work was supported by the Russian Science Foundation (RSF), grant No. 19-72-20125-II. The authors thank the staff of the “Centre for X-ray Diffraction Studies” and the “Centre for Physical Methods of Surface Investigation” of the Research Park at Saint Petersburg State University for their assistance with XPS, XRD, and XRR measurements. We also gratefully acknowledge the National Research Center “Kurchatov Institute” for providing access to the ESCA laboratory facilities and for their valuable technical support, which greatly contributed to this research.

References

- [1] A.D. Akhsakhalyan, E.B. Kluenkov, A.Y. Lopatin, V.I. Luchin, A.N. Neschay, A.E. Pestov, V.N. Polkovnikov, N.N. Salashchenko, M. V. Svechnikov, M.N. Toropov, N.N. Tsybin, N.I. Chkhalo, A. V. Shcherbakov, Current status and development prospects for multilayer X-ray optics at the Institute for Physics of Microstructures, Russian Academy of Sciences, *Journal of Surface Investigation* 11 (2017) 1–19. <https://doi.org/10.1134/S1027451017010049>.
- [2] W. Fornaciari, D. Soudris, Harnessing performance variability in embedded and high-performance many/multi-core platforms: A cross-layer approach, Springer International Publishing, 2018. <https://doi.org/10.1007/978-3-319-91962-1>.
- [3] T. Manouras, P. Argitis, High sensitivity resists for EUV lithography: A review of material design strategies and performance results, *Nanomaterials* 10 (2020) 1–24. <https://doi.org/10.3390/nano10081593>.
- [4] B. Wu, A. Kumar, Extreme ultraviolet lithography and three dimensional integrated circuit - A review, *Appl Phys Rev* 1 (2014). <https://doi.org/10.1063/1.4863412>.
- [5] A. Malik, P. Debacker, G. McIntyre, R.-H. Kim, K. Ronse, EUVL Gen 2.0: Key requirements for constraining semiconductor cost in advanced technology node manufacturing, in: Extreme Ultraviolet (EUV) Lithography IX, 2018. <https://doi.org/10.1117/12.2297447>.
- [6] N. Fu, Y. Liu, X. Ma, Z. Chen, EUV Lithography: State-of-the-Art Review, *Journal of Microelectronic Manufacturing* 2 (2019) 1–6. <https://doi.org/10.33079/jomm.19020202>.
- [7] V. Bakshi, H. Mizoguchi, T. Liang, A. Grenville, J. Benschop, Special Section Guest Editorial: EUV Lithography for the 3-nm Node and Beyond, *Journal of Micro/Nanolithography, MEMS, and MOEMS* 16 (2017) 1. <https://doi.org/10.1117/1.jmm.16.4.041001>.
- [8] A. Sasaki, K. Nishihara, A. Sunahara, H. Furukawa, T. Nishikawa, F. Koike, Theoretical investigation of the spectrum and conversion efficiency of short wavelength extreme-ultraviolet light sources based on terbium plasmas, *Appl Phys Lett* 97 (2010). <https://doi.org/10.1063/1.3524494>.
- [9] T. Otsuka, D. Kilbane, J. White, T. Higashiguchi, N. Yugami, T. Yatagai, W. Jiang, A. Endo, P. Dunne, G. O’Sullivan, Rare-earth plasma extreme ultraviolet sources at 6.5–6.7 nm, *Appl Phys Lett* 97 (2010). <https://doi.org/10.1063/1.3490704>.
- [10] S.A. Garakhin, V.N. Polkovnikov, N.I. Chkhalo, On the Possibilities of Multilayer Mirrors for Measuring the Concentration of Boron Impurities in Diamond, *Journal of Surface Investigation* 13 (2019) 173–176. <https://doi.org/10.1134/S1027451019020071>.
- [11] G. V. Pashkova, A.G. Revenko, A review of application of total reflection X-Ray fluorescence spectrometry to water analysis, *Appl Spectrosc Rev* 50 (2015) 443–472. <https://doi.org/10.1080/05704928.2015.1010205>.

- [12] N. V. Alov, Total reflection X-ray fluorescence analysis: Physical foundations and analytical application (A review), *Inorganic Materials* 47 (2011) 1487–1499. <https://doi.org/10.1134/S0020168511140020>.
- [13] A.A. Akhsakhalyan, Y.A. Vainer, S.A. Garakhin, K.A. Elina, P.S. Zavertkin, S.Y. Zuev, D. V. Ivlyushkin, A.N. Nechay, A.D. Nikolenko, D.E. Pariev, R.S. Pleshkov, V.N. Polkovnikov, N.N. Salashchenko, M. V. Svechnikov, N.I. Chkhalo, Set of Multilayer X-Ray Mirrors for a Double-Mirror Monochromator Operating in the Wavelength Range of 0.41–15.5 nm, *Journal of Surface Investigation* 13 (2019) 1–7. <https://doi.org/10.1134/S1027451019010026>.
- [14] P.C. Uzoma, S. Shabbir, H. Hu, P.C. Okonkwo, O. V. Penkov, Multilayer reflective coatings for beuv lithography: A review, *Nanomaterials* 11 (2021). <https://doi.org/10.3390/nano11112782>.
- [15] T. Otsuka, B. Li, C. O’Gorman, T. Cummins, D. Kilbane, T. Higashiguchi, N. Yugami, W. Jiang, A. Endo, P. Dunne, G. O’Sullivan, A 6.7-nm beyond EUV source as a future lithography source, in: *Extreme Ultraviolet (EUV) Lithography III*, SPIE, 2012: p. 832214. <https://doi.org/10.1117/12.916351>.
- [16] E. Louis, I. Makhot kin, E. Zoet hout, S. ephan Müllender, F. Bij kerk, Multilayer Development for Extreme Ultraviolet and Shorter Wavelength Lithography, n.d.
- [17] V.Y. Banine, K.N. Koshelev, G.H.P.M. Swinkels, Physical processes in EUV sources for microlithography, *J Phys D Appl Phys* 44 (2011). <https://doi.org/10.1088/0022-3727/44/25/253001>.
- [18] R.A. Shaposhnikov, N.V. Zagainov, V.N. Polkovnikov, N.I. Chkhalo, S.A. Garakhin, S.Y. Zuev, MP3 на основе бора - ЖТФ-8-2024, *ЖТФ* 94 (2024) 1260–1268. <https://doi.org/10.61011/JTF.2024.08.58553.119-24>.
- [19] N I Chkhalo, New Concept for the Development of High-Performance X-ray Lithography, *Микроэлектроника* 53 (2024) 375–388. <https://doi.org/10.1134/S1063739724600511>.
- [20] N.I. Chkhalo, I. V Malyshev, A.E. Pestov, V.N. Polkovnikov, N.N. Salashchenko, M.N. Toropov, Diffraction limited X-ray optics: technology, metrology, applications, *Physics-Uspekhi* 63 (2020) 67–82. <https://doi.org/10.3367/ufne.2019.05.038601>.
- [21] Q. Huang, Y. Liu, Y. Yang, R. Qi, Y. Feng, I. V. Kozhevnikov, W. Li, Z. Zhang, H. Jiang, L. Zhang, A. Li, J. Wang, Z. Wang, Nitridated Ru/B4C multilayer mirrors with improved interface structure, zero stress, and enhanced hard X-ray reflectance, *Opt Express* 26 (2018) 21803. <https://doi.org/10.1364/oe.26.021803>.
- [22] C. Borel, C. Morawe, A. Rommeveaux, C. Huguenot, J.-C. Peffen, Reflectivity and stress responses of multilayers upon isothermal treatment, in: *Advances in X-Ray/EUV Optics, Components, and Applications*, SPIE, 2006: p. 63170I. <https://doi.org/10.1117/12.678472>.
- [23] C. Borel, C. Morawe, E. Ziegler, T. Bigault, J.-Y. Massonnat, J.-C. Peffen, E. Debourg, In situ study of multilayer reflectivity upon heat treatment under synchrotron radiation, in: *Laser-Generated, Synchrotron, and Other Laboratory X-Ray and EUV Sources, Optics, and Applications II*, SPIE, 2005: p. 591801. <https://doi.org/10.1117/12.613873>.
- [24] R.A. Shaposhnikov, V.N. Polkovnikov, N.I. Chkhalo, S.A. Garakhin, Study of structural and reflective characteristics of multilayer X-ray mirrors based on a pair of Ru/B materials, *Technical Physics Letters* 51 (2025). <https://doi.org/10.61011/TPL.2025.01.60138.20075>.
- [25] D.G. Stearns, R.S. Rosen, S.P. Vernon, Normal-incidence x-ray mirror for 7 nm, 1991. <https://doi.org/10.1364/ol.16.001283>.
- [26] V. V. Lider, Multilayer X-ray interference structures, *Uspekhi Fizicheskikh Nauk* 189 (2019) 1137–1171. <https://doi.org/10.3367/ufnr.2018.10.038439>.

- [27] D. Ksenzov, C. Schlemper, U. Pietsch, Resonant soft x-ray reflectivity of Me/B4C multilayers near the boron K edge, 2010. <https://doi.org/10.1364/AO.49.004767>.
- [28] T.D. Nguyen, R. Gronsky, J.B. Kortright, Microstructure-Roughness Interrelation In Ru/C and Ru/B4C X-Ray Multilayers, 1993. <https://doi.org/10.1557/PROC-280-161>.
- [29] N.I. Chkhalo, S. Künstner, V.N. Polkovnikov, N.N. Salashchenko, F. Schäfers, S.D. Starikov, High performance La/B4C multilayer mirrors with barrier layers for the next generation lithography, *Appl Phys Lett* 102 (2013). <https://doi.org/10.1063/1.4774298>.
- [30] S. Bajt, J. Alameda, T. Barbee, W.M. Clift, J.A. Folta, B. Kaufmann, E. Spiller, Improved reflectance and stability of Mo/Si multilayers, 2001. <https://doi.org/10.1111/12.450946>.
- [31] V.N. Polkovnikov, N.N. Salashchenko, M. V. Svechnikov, N.I. Chkhalo, Beryllium-based multilayer X-ray optics, *Uspekhi Fizicheskikh Nauk* 190 (2020) 92–106. <https://doi.org/10.3367/ufnr.2019.05.038623>.
- [32] S. Hufner, *Photoelectron Spectroscopy*, third ed., Springer-Verlag, Berlin, 2003.
- [33] N. Mårtensson, J. Söderstrom, S. Svensson, O. Travnikova, M. Patanen, C. Miron, L.J. Sæthre, K.J. Borve, T.D. Thomas, J.J. Kas, F.D. Vila, J.J. Rehr, On the relation between X-ray photoelectron spectroscopy and XAFS, in: *J Phys Conf Ser*, Institute of Physics Publishing, 2013. <https://doi.org/10.1088/1742-6596/430/1/012131>.
- [34] S. Tougaard, Low energy inelastic electron scattering properties of noble and transition metals, 1987. [https://doi.org/10.1016/0038-1098\(87\)90166-9](https://doi.org/10.1016/0038-1098(87)90166-9).
- [35] S. Tougaard, Practical algorithm for background subtraction, 1989. [https://doi.org/10.1016/0039-6028\(89\)90380-4](https://doi.org/10.1016/0039-6028(89)90380-4).
- [36] CasaXPS: Processing Software for XPS, AES, SIMS and More, <Http://Casaxps.Com> (2022).
- [37] D.L. Windt, IMD—Software for modeling the optical properties of multilayer films, *Computers in Physics* 12 (1998) 360–370. <https://doi.org/10.1063/1.168689>.
- [38] M. Svechnikov, Multifitting: Software for the reflectometric reconstruction of multilayer nanofilms, *J Appl Crystallogr* 53 (2020) 244–252. <https://doi.org/10.1107/S160057671901584X>.
- [39] A. Jain, S.P. Ong, G. Hautier, W. Chen, W.D. Richards, S. Dacek, S. Cholia, D. Gunter, D. Skinner, G. Ceder, K.A. Persson, Commentary: The materials project: A materials genome approach to accelerating materials innovation, *APL Mater* 1 (2013). <https://doi.org/10.1063/1.4812323>.
- [40] D. V. Suetin, I.R. Shein, Electronic Structure, Mechanical and Dynamical Stability of Hexagonal Subcarbides M2C (M = Tc, Ru, Rh, Pd, Re, Os, Ir, and Pt): Ab Initio Calculations, *Physics of the Solid State* 60 (2018) 213–224. <https://doi.org/10.1134/S1063783418020282>.
- [41] W.D. Richards, L.J. Miara, Y. Wang, J.C. Kim, G. Ceder, Interface Stability in Solid-State Batteries, *Chemistry of Materials* 28 (2016) 266–273. <https://doi.org/10.1021/acs.chemmater.5b04082>.
- [42] Y. Xiao, Y. Wang, S.H. Bo, J.C. Kim, L.J. Miara, G. Ceder, Understanding interface stability in solid-state batteries, *Nat Rev Mater* 5 (2020) 105–126. <https://doi.org/10.1038/s41578-019-0157-5>.
- [43] D.J. Morgan, Resolving ruthenium: XPS studies of common ruthenium materials, *Surface and Interface Analysis* 47 (2015) 1072–1079. <https://doi.org/10.1002/sia.5852>.
- [44] R. Kotz, H.J. Lewerenz, S. Stucki, XPS Studies of Oxygen Evolution on Ru and RuO₂ Anodes, 1983. <https://doi.org/10.1149/1.2119829>.

[45] M.K. Kolel-Veetil, R.M. Gamache, N. Bernstein, R. Goswami, S.B. Qadri, K.P. Fears, J.B. Miller, E.R. Glaser, T.M. Keller, Substitution of silicon within the rhombohedral boron carbide (B4C) crystal lattice through high-energy ball-milling, *J Mater Chem C Mater* 3 (2015) 11705–11716. <https://doi.org/10.1039/c5tc02956b>.

[46] R. Bao, D.B. Chrisey, Chemical states of carbon in amorphous boron carbide thin films deposited by radio frequency magnetron sputtering, *Thin Solid Films* 519 (2010) 164–168. <https://doi.org/10.1016/j.tsf.2010.07.090>.

[47] S.S. Sakhonenkov, A. V. Bugaev, R.A. Shaposhnikov, V.N. Polkovnikov, E.O. Filatova, Chemical interactions at interfaces in nanoscale Mo/B4C multilayered structures, *Surfaces and Interfaces* 55 (2024). <https://doi.org/10.1016/j.surfin.2024.105467>.

[48] L. Chen, T. Goto, T. Hirai, State of boron in chemical vapour-deposited SiC-B composite powders, *Journal of materials science letters*, 1990.

[49] V. N. Polkovnikov, R. A. Shaposhnikov, N. I. Chkhalo, N. N. Salashchenko, N. A. Dyuzhev, F. A. Pudonin, G. D. Demin, Y-based multilayer mirrors for the spectral range of 8–12 nm, n.d. <https://doi.org/10.3103/S1068335621120101>.

[50] Lider V. V., Focusing diffraction optics for orbital telescopes, *Opt Spectrosc* 130 (2022) 855–878. <https://doi.org/10.21883/eos.2022.07.54725.44-22>.

[51] D.S. Kvashennikov, Y.A. Vainer, S.Y. Zuev, V.N. Polkovnikov, Internal Stresses in Mo/Y Multilayer Mirrors, *Journal of Surface Investigation* 13 (2019) 177–181. <https://doi.org/10.1134/S1027451019020113>.

[52] S.S. Sakhonenkov, E.O. Filatova, A.U. Gaisin, S.A. Kasatikov, A.S. Konashuk, R.S. Pleshkov, N.I. Chkhalo, Angle resolved photoelectron spectroscopy as applied to X-ray mirrors: An in depth study of Mo/Si multilayer systems, *Physical Chemistry Chemical Physics* 21 (2019) 25002–25010. <https://doi.org/10.1039/c9cp04582a>.

[53] V. Sisodia, D. Kabiraj, W. Bolse, I.P. Jain, Phase formation by ion beam mixing in the Ti/Si multilayer system, in: *Appl Surf Sci*, Elsevier, 2006: pp. 4016–4019. <https://doi.org/10.1016/j.apsusc.2005.09.035>.

[54] S. Ramaswamy, C. Gopalakrishnan, K.R. Ganesh, K. Jeganathan, M. Ponnavaikko, Effects of argon ion bombardment on the structure and magnetic properties of ultrathin Fe films, *Journal of Vacuum Science & Technology B, Nanotechnology and Microelectronics: Materials, Processing, Measurement, and Phenomena* 28 (2010) 795–798. <https://doi.org/10.1116/1.3457935>.

[55] A. Barna, M. Menyhard, G. Zsolt, A. Koos, A. Zalar, P. Panjan, Interface broadening due to Ar⁺ ion bombardment measured on Co/Cu multilayer at grazing angle of incidence, *Journal of Vacuum Science & Technology A: Vacuum, Surfaces, and Films* 21 (2003) 553–557. <https://doi.org/10.1116/1.1559921>.

[56] D.D. Sarma, R. Rao, XPES studies of oxides of second- and third-row transition metals including rare earths, 1980. [https://doi.org/10.1016/0368-2048\(80\)85003-1](https://doi.org/10.1016/0368-2048(80)85003-1).

[57] A. Ohyoshi, F. Gotzfried, W. Beck, Polynuclear carbonyl complexes of ruthenium and osmium with methylhiolate and bromide bridging ligands, 1980. <https://doi.org/10.1246/cl.1980.1537>.

[58] Y. Kaga, Y. Abe, H. Yanagisawa, M. Kawamura, K. Sasaki, Ru and RuO₂ Thin Films by XPS, *Surface Science Spectra* 6 (1999) 68–74. <https://doi.org/10.1116/1.1247890>.

[59] C.L. Bianchi, V. Ragaini, M.G. Cattania, An XPS study on ruthenium compounds and catalysts, 1991. [https://doi.org/10.1016/0254-0584\(91\)90025-P](https://doi.org/10.1016/0254-0584(91)90025-P).

[60] K.S. Kim, N. Winograd, X-Ray Photoelectron Spectroscopic Studies of Ruthenium-Oxygen Surfaces, 1974. [https://doi.org/10.1016/0021-9517\(74\)90184-5](https://doi.org/10.1016/0021-9517(74)90184-5).

[61] J. Hrbek, D.G. van Campen, I.J. Malik, The early stages of ruthenium oxidation, *Journal of Vacuum Science & Technology A: Vacuum, Surfaces, and Films* 13 (1995) 1409–1412. <https://doi.org/10.1116/1.579573>.

[62] R. Escamilla, E. Carvajal, M. Cruz-Irisson, F. Morales, L. Huerta, E. Verdin, XPS study of the electronic density of states in the superconducting Mo₂B and Mo₂BC compounds, *J Mater Sci* 51 (2016) 6411–6418. <https://doi.org/10.1007/s10853-016-9938-z>.

[63] R.J. Colton, J. Wayne. Rabalais, Electronic structure to tungsten and some of its borides, carbides, nitrides, and oxides by x-ray electron spectroscopy, *Inorg Chem* 15 (1976) 236–238. <https://doi.org/10.1021/ic50155a049>.

[64] W.A. Brainard, D.R. Wheeler, An XPS study of the adherence of refractory carbide silicide and boride rf-sputtered wearresistant coatings, *J Vac Sci Technol* 15 (1978) 1800–1805. <https://doi.org/10.1116/1.569845>.

[65] A.D. Yaprutsev, A.Y. Bykov, A.E. Baranchikov, K.Y. Zhizhin, V.K. Ivanov, N.T. Kuznetsov, closo-Dodecaborate Intercalated Yttrium Hydroxide as a First Example of Boron Cluster Anion-Containing Layered Inorganic Substances, *Inorg Chem* 56 (2017) 3421–3428. <https://doi.org/10.1021/acs.inorgchem.6b02948>.

[66] V. V. Avdeeva, E.A. Malinina, I.B. Sivaev, V.I. Bregadze, N.T. Kuznetsov, Silver and copper complexes with closo-polyhedral borane, carborane and metallacarborane anions: Synthesis and X-ray structure, *Crystals (Basel)* 6 (2016). <https://doi.org/10.3390/crust6050060>.

[67] S.Y. Zuyev, D.E. Pariev, R.S. Pleshkov, V.N. Polkovnikov, N.N. Salashchenko, M. V. Svechnikov, M.G. Sertsu, A. Sokolov, N.I. Chkhalo, F. Schäfers, Mo/Si Multilayer Mirrors with B4C and Be Barrier Layers, *Journal of Surface Investigation* 13 (2019) 169–172. <https://doi.org/10.1134/S1027451019020216>.

[68] S. Braun, H. Mai, M. Moss, R. Scholz, A. Leson, Mo/Si multilayers with different barrier layers for applications as extreme ultraviolet mirrors, *Japanese Journal of Applied Physics, Part 1: Regular Papers and Short Notes and Review Papers* 41 (2002) 4074–4081. <https://doi.org/10.1143/jjap.41.4074>.

[69] V.N. Polkovnikov, N.N. Salashchenko, S.D. Starikov, N.I. Chkhalo, High performance multilayer La/B4C mirrors with carbon barrier layers, *Bulletin of the Russian Academy of Sciences: Physics* 78 (2014) 61–63. <https://doi.org/10.3103/S1062873814010146>.

[70] M.N. Drozdov, Y.N. Drozdov, N.I. Chkhalo, V.N. Polkovnikov, N.N. Salashchenko, P.A. Yunin, V. V. Roddatis, A. Tolstogouzov, The role of ultra-thin carbon barrier layers for fabrication of La/B4C interferential mirrors: Study by time-of-flight secondary ion mass spectrometry and high-resolution transmission electron microscopy, *Thin Solid Films* 577 (2015) 11–16. <https://doi.org/10.1016/j.tsf.2015.01.025>.

[71] V.I.T.A. De Rooij-Lohmann, L.W. Veldhuizen, E. Zoethout, A.E. Yakshin, R.W.E. Van De Kruijs, B.J. Thijssse, M. Gorgoi, F. Schäfers, F. Bijkerk, Chemical interaction of B4C, B, and C with Mo/Si layered structures, *J Appl Phys* 108 (2010). <https://doi.org/10.1063/1.3503521>.

[72] J.I. Larruquert, Reflectance enhancement in the extreme ultraviolet and soft x rays by means of multilayers with more than two materials, *J. Opt. Soc. Am. A*, 19 (2), 2002. <https://doi.org/10.1364/JOSAA.19.000391>.

[73] J.I. Larruquert, General theory of sub-quarterwave multilayers with highly absorbing materials, *J. Opt. Soc. Am. A*, 18 (10), 2001. <https://doi.org/10.1364/josaa.18.002617>.

- [74] Yang Liu, Qiushi Huang, Runze Qi, Yufei Feng, Zhong Zhang, Guangzhi Yin, Xingmin Zhang, Hui Jiang, Zhanshan Wang, Thermal and temporal stability of the nitridated Ru/B4C multilayer for high-flux monochromator application, *Appl Opt* 59 (2020) 48–53. <https://doi.org/10.1364/AO.59.000A48>.
- [75] M. Barthelmess, S. Bajt, Thermal stability on Mo/B4C multilayers, in: *Damage to VUV, EUV, and X-Ray Optics III*, SPIE, 2011: p. 807710. <https://doi.org/10.1117/12.886751>.
- [76] M. Barthelmess, S. Bajt, Thermal and stress studies of normal incidence Mo/B4C multilayers for a 6.7 nm wavelength, 2011. <https://doi.org/10.1364/AO.50.001610>.
- [77] J. Eastman, P. Baumeister, The microstructure of polished optical surfaces, 1974. [https://doi.org/10.1016/0030-4018\(74\)90135-7](https://doi.org/10.1016/0030-4018(74)90135-7).
- [78] Springer Materials the Landolt-Börnstein database, <Https://Engineering.Library.Cornell.Edu/Database/Springer-Materials-the-Landolt-Bornstein-Database/> (n.d.).